# Influence of eccentricity of H-shaped steel in soil-cement wall on vertical bearing capacity

R. Kiritani.
*KONOIKE CONSTRUCTION CO., LTD., Tsukuba, Japan, kiritani_ry@konoike.co.jp*

S. Shimomura.
*Nihon University, Narashino, Japan, shimomura.shuichi@nihon-u.ac.jp*

**ABSTRACT:** Soil-cement walls are a type of earth-retaining wall constructed by inserting H-shaped steel beams into soil-cement, which is made by mixing in-situ soil with a cement-based suspension. While earth-retaining walls are primarily expected to resist horizontal soil-water pressure, vertical bearing capacity is also required when using top-down construction methods or ground anchoring, or when the earth-retaining wall is used as a wall pile. When evaluating the vertical bearing capacity of an earth-retaining wall, consideration must be given not only to the vertical bearing capacity of the soil, but also to the bond resistance and shear resistance between the steel and the soil-cement and the bearing resistance of the soil-cement at the tip of the steel. Although H-shaped steel beams can be eccentric within the soil-cement cross section due to installation inaccuracy, the effect of steel eccentricity on vertical bearing capacity has not been investigated. Therefore, in this study, we conducted vertical loading tests on a cylindrical model pile using a pressurized tank. The model pile was extracted from one of the columns of a soil-cement wall (a row with several columns). The results confirm that the eccentricity of the steel reduces the bond resistance, shear resistance, and bearing resistance, but increases the residual bond resistance and shear resistance.

## 1 INTRODUCTION

Soil-cement walls, which are constructed to prevent ground collapse and reduce the impact on adjacent structures during basement construction, are temporary structures designed to resist horizontal earth pressure and intercept water. However, the vertical bearing capacity must be considered when vertical loads are to be borne when using top-down construction methods or ground anchoring, or when the earth-retaining wall is used as a wall pile. Because the vertical load is transmitted from H-shaped steel beams to the ground through soil-cement, the vertical bearing capacity is evaluated based on the bearing capacity of the ground or the wall strength, whichever is lower. The strength of the soil-cement used in retaining walls is 0.5 to 2.0 N/mm$^2$, which is lower than that of precast or cast-in-place concrete piles. It is thus important to evaluate the vertical bearing capacity based on the wall strength.

In Japan, this capacity is generally determined by adding the bond and shear resistance of the H-shaped steel and soil-cement to the bearing resistance of the soil-cement to the H-shaped steel. The bearing capacity of soil-cement walls has been extensively investigated. Abe et al. (2018) and Taya et al. (2021) conducted in-situ vertical loading tests, and Satake et al. (2003), Sato et al. (2003), Tsuchiya et al. (2004), and Watanabe et al. (2021) conducted vertical loading tests on model piles with ground confinement simulated using steel or acrylic pipes. However, a quantitative evaluation of the effect of ground confinement on the assessment of vertical bearing capacity based on wall strength was not conducted and the detailed support mechanism was unclear. Therefore, Kiritani et al. (2025) conducted vertical loading tests on a model pile from which one element of a soil-cement wall was extracted from a ground model. The results were compared with those of unconfined loading tests in air. It was found that the shear and bearing resistances increased owing to the ground confinement effect. However, due to installation inaccuracy, the H-shaped steel may be eccentric within the soil-cement cross section. Nevertheless, the effect of H-shaped steel eccentricity on the vertical bearing capacity has not yet been investigated.

Therefore, we conducted vertical loading tests on a cylindrical model pile using a pressurized tank. The model pile was extracted from one of the columns of a soil-cement wall. The effect of the H-shaped steel eccentricity on the vertical bearing capacity was investigated.

## 2 VERTICAL BEARING MECHANISM

Figure 1 illustrates the process of vertical load transfer to a soil-cement wall. Vertical loads are transferred from the H-shaped steel to the ground through the soil-cement. This load is shared by the bond resistance between the H-shaped steel and the soil-cement, the shear resistance of the soil-cement, and the bearing resistance of the soil-cement below the H-shaped steel. Vertical loads transmitted from the soil-cement to the ground are supported by the skin friction between the soil-cement and the ground and the tip resistance of the wall.

Figure 2 shows the two fracture modes between H-shaped steel and soil-cement. Figure 2(a) shows H-shaped bond failure of the steel and soil-cement, wherein the soil-cement at the tip of the steel is compressed by the cross section of the steel. Figure 2(b) shows the bond and shear failures in the shape of a rectangle enclosing the steel, wherein the soil-cement below the bottom of the steel is compressed by the closed cross section of the steel.

In Japan, the vertical bearing capacity is determined from the wall strength, as indicated in the AIJ Recommendations for Design of Earth Retaining for Excavation (2017), as follows:

$$R_a = min\,\{f_a \cdot \psi_{a1} \cdot L_h + f_c \cdot A_h,\; (f_a \cdot \psi_{a2} + f_s \cdot \psi_s)L_h + f_c \cdot A_{hp}\} \quad (1)$$

$$f_a = F_c/10F_s \quad (2\text{-}1)$$

$$f_c = F_c/F_s \quad (2\text{-}2)$$

$$f_s = F_c/3F_s \quad (2\text{-}3)$$

where $R_a$ is the vertical bearing capacity (kN) determined from the wall strength; $f_a$ is the allowable bond stress (kN/m$^2$) of the soil-cement; $\Psi_{a1}$, $L_h$, and $A_h$ are the perimeter (m), length (m), and cross-sectional area (m$^2$) of the steel, respectively; $f_c$ is the allowable compressive stress (kN/m$^2$) for the soil-cement; $\Psi_{a2}$ is the length (m) of the closed cross section of the steel where the bond is considered; $f_s$ is the allowable shear stress (kN/m$^2$) for the soil-cement; $\Psi_s$ is the length (m) of the closed cross section of the steel where the shear stress is considered; $A_{hp}$ is the closed cross-sectional area (m$^2$) of the steel; $F_c$ is the design strength (kN/m$^2$) of the soil-cement; and $F_s$ is a safety factor (=2.0).

As shown in Equation (1), $R_a$ is a simple summation of the bond resistance or the bond and shear resistance between the steel and the soil-cement and the bearing resistance of the tip of the steel. As shown in Equations (2-1) to (2-3), the allowable stress for each case is evaluated using the design strength based on the unconfined compressive strength of the soil-cement. Because soil-cement walls are constructed within the ground, their vertical bearing capacity may increase because of suppression of deformation as a result of the confining pressure in the ground; however, this is not considered in Equation (1). Additionally, due to installation inaccuracy, the H-shaped steel of a soil-cement wall may be eccentric, which may affect the vertical bearing capacity. Therefore, this study investigates the effects of ground confinement and H-shaped eccentricity on the vertical bearing capacity of soil-cement walls.

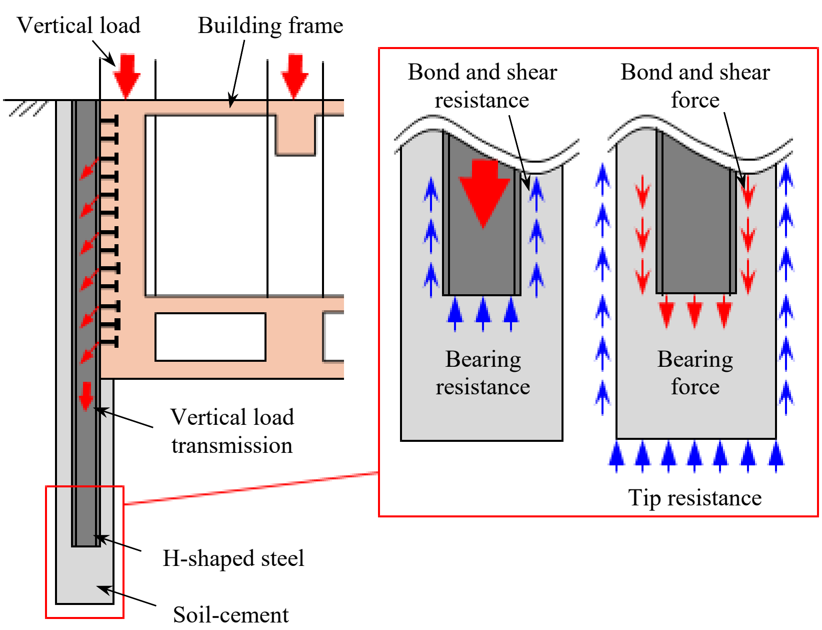


*Figure 1. Diagram of vertical load transmission*

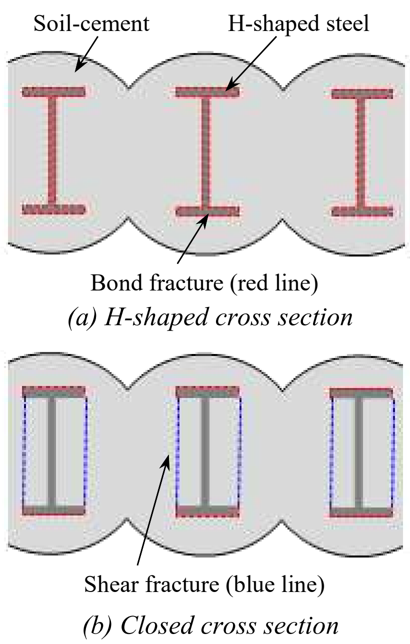


*Figure 2. Fracture modes*

## 3 EXPERIMENTAL

Table 1 lists the experimental conditions and Figure 3 shows an illustration of the model piles with eccentric H-shaped steel. The model pile with the steel placed in the center was based on the experimental results of Kiritani et al. (2025). For the case labels in Table 1, "e" indicates eccentric arrangement and "O", "S", "H", and "C" indicate the subject of evaluation. The letter after the hyphen indicates whether the vertical loading tests were conducted in an unconfined condition (U) or in the model ground (G). The steel of the model pile was H-shaped stainless steel (H-50 × 50 × 4 × 4 mm). The diameter of the soil-cement section was 100 mm, the bond length between the steel and the soil-cement (hereafter referred to as the bond part) was 190 mm, and the length of the soil-cement section below the steel (hereafter referred to as the bearing part) was 200 mm. The e-series assumes conditions where the eccentricity of the steel was at its maximum (i.e., the steel was 18.3 mm from the center of the soil-cement section).

The O-series was used to evaluate the vertical bearing capacity of model piles where both the bond part and the bearing part resist vertical loading (Figure 3(a)). The S-series pile was the O-series pile with the soil-cement below the steel removed to evaluate the bond and shear resistances. Additionally, an acrylic plate with a hollow center (acrylic part: diameter × height =100 × 20 mm; hollow part: width × depth × height =55 × 55 × 10 mm) was placed at the tip of the pile to allow the steel to push through (Figure 3(b)). The H-series was used to evaluate the bearing resistance of the H-shaped cross section. The bond between the steel and the soil-cement was eliminated using Teflon sheets and grease (Figure 3(c)). In the C-series, an iron plate was bonded to the bond part to simulate a closed cross section and the bearing resistance of the closed cross section was evaluated. The bond around the periphery of the closed cross section was eliminated, similar to that in the H-series (Figure 3(d)). In the model ground of the H- and C-series piles, Teflon sheets, grease, and rubber membranes were installed around the periphery of the model pile to prevent tensile failure of the soil-cement at the tip of the H-shaped steel. Additionally, skin friction was eliminated in the region where the bond was eliminated.

Table 2 lists the blending conditions for the soil-cement. The target unconfined compressive strength of the soil-cement was set to 2.0 N/mm$^2$.

The following procedure was employed to construct the model piles:

*Table 1. Test conditions*

| Case | Position of H-shaped steel | Valuation objects | Overburden pressure (kPa) |
|---|---|---|---|
| O-U | Center | Original model | Unconfined |
| O-G | | | 100 |
| eO-G | Eccentricity | | |
| S-U | Center | Bond and shear resistance | Unconfined |
| S-G | | | 100 |
| eS-G | Eccentricity | | |
| H-U | Center | H-shaped cross section bearing resistance | Unconfined |
| H-G | | | 100 |
| eH-G | Eccentricity | | |
| C-U | Center | Closed cross section bearing resisitance | Unconfined |
| C-G | | | 100 |
| eC-G | Eccentricity | | |

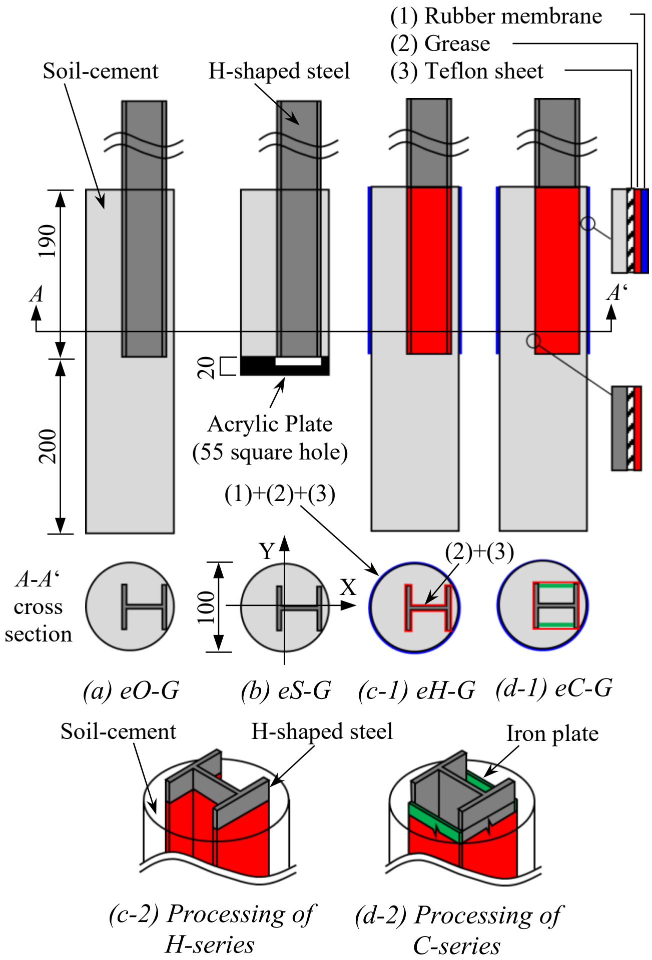


*Figure 3. Test piles (e-series)* (Unit: mm)

*Table 2. Blending conditions for soil-cement*

| Design strength (N/mm$^2$) | Soil: Soil sample | Soil: Water content (%) | Cement slarry: Cement-based soildifying material (%) | Cement slarry: W/C (%) | Cement slarry: Bentonite (%) |
|---|---|---|---|---|---|
| 2.0 | Tohoku silica sand No.5 | 18 | 20 | 60 | 5 |

- Tohoku Silica Sand No. 5 was mixed with tap water to prepare sample soil.
- After the cement-based solidifying material was mixed with bentonite, tap water was added and the mixture was stirred to form a cement slurry.
- The soil-cement slurry was prepared by mixing the sample soil and cement slurry using a mixer.
- The H-shaped steel was inserted into a steel mold and the pile was placed on a curing table with the pile head facing downward.
- The soil-cement slurry was poured into a steel mold seal and cured for 7 d at 20 °C.

During the construction of the model piles, an additional layer of the soil-cement, measuring approximately 10% of the pile length, was added to the pile tip and excess material was cut after curing. The unconfined compression strength of the mix, made on the day of model pile construction, was 1.8 to 2.3 $N/mm^2$ after 7 d of curing.

Figure 4 shows an overview of the vertical loading test apparatus and pressurized tank, which had an inner diameter of 795 mm and an inner height of 1000 mm. The height of the soil samples in the tank was 890 mm. The friction on the inner tank wall was minimized using Teflon sheets, grease, and rubber membranes.

Figure 5 shows grain size distribution curves for the Toyoura sand used to construct the model ground and the Tohoku Silica Sand No. 5 used for the model pile. The ground model was prepared using Toyoura sand and air pluviation through a sand rainer. The target relative density was 80%.

The procedure for the pressurized-soil-tank experiment was as follows:

- Toyoura sand was retained at the depth of the model pile installation inside the pressurized tank.
- The surface where the model pile was to be placed was leveled, the pile was placed in the center of the pressurized tank, the Toyoura sand was rained down again, and the pressur-ized surface was leveled.
- A rubber sheet and a pressurized plate were placed on the pressurized surface and four load cells. Two displacement transducers were installed to control the overburden pressure on the pressurized plate and four displacement transducers were installed to measure the changes in the position at the pile head and soil-cement top edge.
- After the overburden pressure was applied, the pile was allowed to rest until the subsidence reached a stable state.
- A screw jack with a load cell was positioned over the center of the H-shaped steel and a vertical load of approximately 1 mm/min was applied.

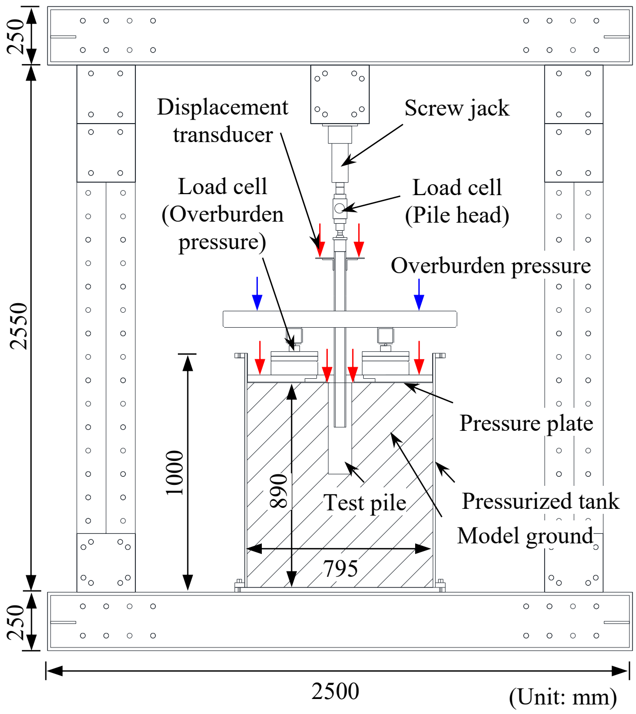


*Figure 4. Test equipment*

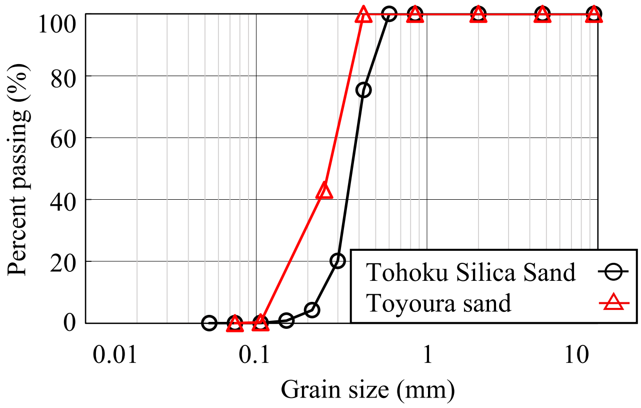


*Figure 5. Grain size distribution curves*

- The load was removed when the pile head displacement reached 10 mm.
- After unloading, the model pile was excavated from the model ground and the fracture characteristics were inspected.

The model ground was subjected to overburden pressure by placing a pressure plate on its surface and manually tightening it using a clamp connected to a well girder. During vertical loading, the ground settled as the model piles were displaced and the applied pressure decreased by approximately 10%. Although the relationship between pressure reduction and settlement varied slightly in each case, this study compared them while ignoring this variation.

The procedure for the in-air experiment was the same as that for the pressurized-soil-tank experiment, except for the ground preparation and overburden-pressure control. The pile was unloaded after the peak pile head load was confirmed. The model pile in the in-air experiment was supported by a rigid steel plate and the boundary conditions at the bottom of the pile differed from those in the pressurized-soil-tank experiment.

## 4 RESULTS AND DISCUSSION

Figure 6 shows the relationship between the pile head load $P$, the pile head displacement $S_P$, and the soil-cement top displacement $S_S$ for the O-series piles. It illustrates two key measurements: the pile head load at the first abrupt change in the $P$ to $S_P$ relationship (hereafter referred to as the pile strength $P_P$) and that under a 10-mm pile head displacement (hereafter referred to as the pile residual strength $P_R$). First, comparing rigidity, that for O-U was the highest, while those for O-G and eO-G were comparable. Because O-G and eO-G were conducted within the model ground, each displacement includes the settlement of the model ground. The difference in stiffness stems from the different boundary conditions at the pile base compared to those for O-U. The $P_P$ value for O-G is higher than that for O-U. As noted in our previous research (Kiritani et al., 2025), this indicates an increase in pile strength due to the confinement effect of the ground. The $P_P$ value for eO-G is lower than that for O-G, indicating a decrease in pile strength due to the eccentricity of the H-shaped steel. A similar reduction in pile strength was noted in the study of Ikeuchi et al. (2024) on cast-in-place piles. The increase in pile strength due to soil confinement stress offsets the decrease in pile strength caused by the steel eccentricity, resulting in a higher $P_P$ value for eO-G compared to that for O-U. Finally, we compare the $P_R$ values. Note that for O-U, due to the absence of confinement from the model ground and differences in boundary conditions, brittle failure occurred after $P_P$ was reached. Therefore, the $P_R$ value for O-U was excluded from the evaluation. For both O-G and eO-G, after $P_P$ was reached, a displacement difference (hereafter referred to as the relative displacement) occurred between $S_P$ and $S_S$, causing the pile head load to decrease. The $P_R$ value for eO-G is higher than that for O-G. The reason for this is explained later with regard to Figure 8.

Figure 7 shows sketches of the O-series pile after a loading test. The pile sketches represent only two orthogonal directions for illustrative purposes. As shown in Figure 6, the O-U pile exhibited virtually no relative displacement during loading, indicating no damage to the bonded joint. Additionally, compressive failure occurred at the pile tip. In contrast, relative displacement occurred in the O-G and eO-G piles after $P_P$ was reached and both bond and shear failure was evident. In the eO-G piles, cracks concentrated in the eccentric direction, with vertical and diagonal cracks occurring from the bond part to the support part. Additionally, the soil-cement was partially detached from the steel tip.

Figure 8 shows the relationship between $P$, $S_P$, and $S_S$ for the S-series piles. The $P_P$ value increases in the order S-U, eS-G, S-G. This magnitude relationship is the same as that for the O-series shown in Figure 6. The increase in bond strength and shear strength due to ground confinement stress offsets the reduction in each type of strength caused by the steel eccentricity, resulting in a higher $P_P$ value for eS-G than that for S-U. Furthermore, for both S-G and eS-G, relative displacement occurred after $P_P$ was reached, causing a decrease in pile head load. As shown later in Figures 10 and 12, the pile head load did not decrease after $P_P$ was reached for the H- and C-series.

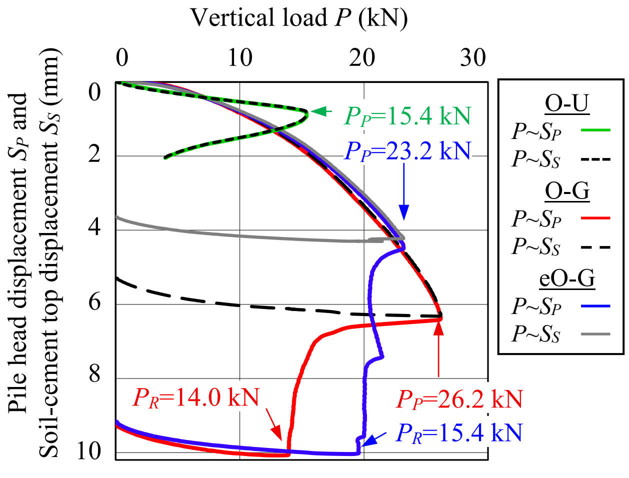


*Figure 6. Relationship between P and S (O-series)*

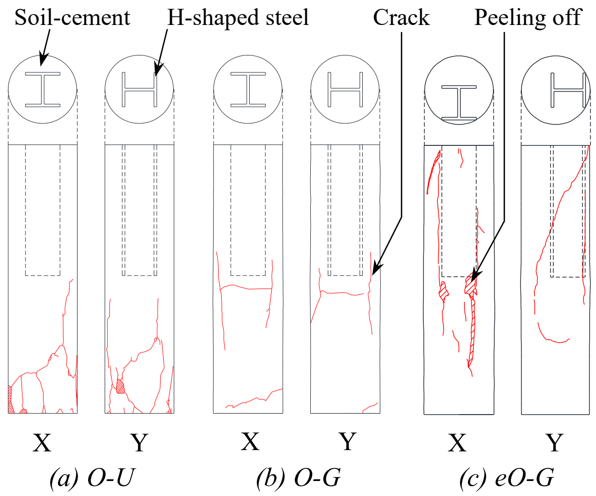


*Figure 7. Sketches of pile after loading test (O-series)*

This indicates that the decrease in $P$ after $P_P$ was reached for O-G and eO-G shown in Figure 6 is due to bond failure and shear failure. The $P_R$ value for eS-G is higher than that for S-G. The residual shear strength increased due to the eccentricity of the steel. This increase in residual shear strength is the reason for the increase in residual strength of the O-series shown in Figure 6.

Figure 9 shows the fracture properties of the S-series piles. The sketch of the S-U pile is not shown because the fractures were severe. Figure 9(a) shows that bond failure occurred on the entire flange outside the closed cross section. Additionally, bond failure was observed in the upper part of the steel, shear failure was observed in the lower part of the steel in the closed cross section, and tensile failure occurred at the boundary between the bond and shear failures.

As shown in Figure 2, two failure modes are possible between the steel and the soil-cement. When the sum of the shear strength and tensile strength is smaller than the bond strength, shear failure occurs. In this experiment, the shear failures at the lower part of the steel occurred at approximately 170, 80, and 140 mm for the S-U, S-G, and eS-G piles, respectively. Our previous study (Kiritani et al., 2025) pointed out that the shear strength increases due to the confinement effect of the ground. For the S-G and eS-G piles confined by the model ground, the shear strength increased and the shear failure zone was smaller than that for the S-U pile. The shear failure zone for eS-G was wider than that for S-G. This occurred because, in the eccentric direction, the distance from the steel to the outer perimeter of the soil-cement was shorter for eS-G, resulting in lower confining pressure on the soil-cement surrounding the steel. Furthermore, as mentioned for Figure 8, the $P_R$ value for eS-G was larger than that for S-G. The wider shear failure zone likely increased the residual shear strength.

Figures 10 to 13 show the relationship between $P$, $S_P$, and $S_S$ for the H- and C-series piles, along with sketches. The magnitude relationships of $P_P$ and $P_R$ for the H- and C-series are similar to those for the O-series.

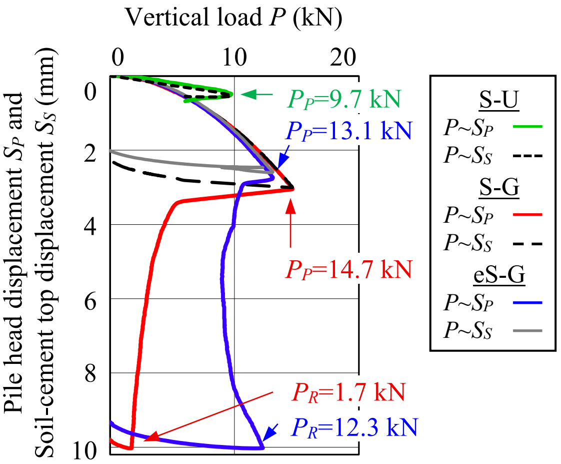


*Figure 8. Relationship between P and S (S-series)*

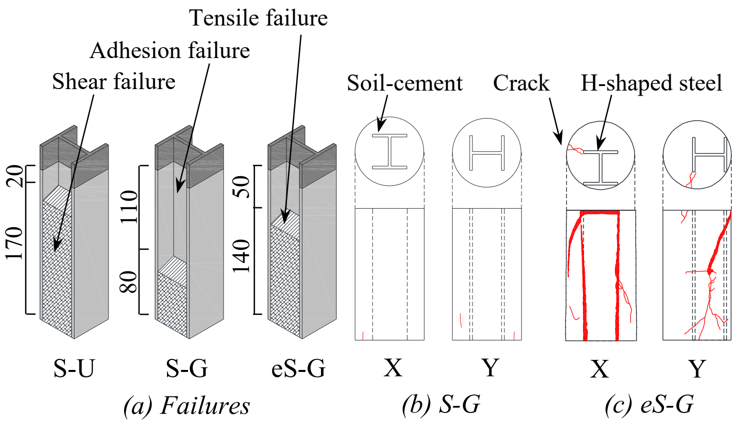


*Figure 9. Sketches of pile after loading test (S-series)*

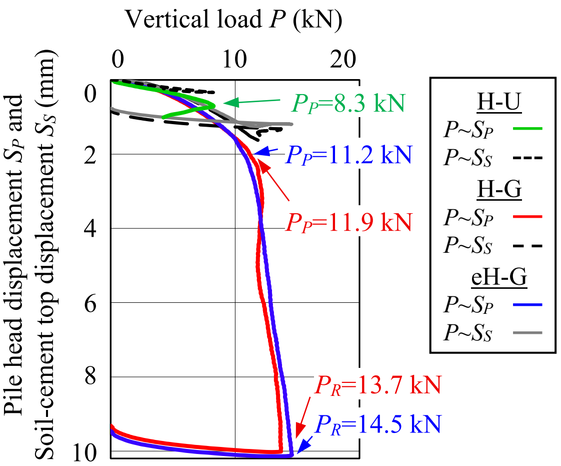


*Figure 10. Relationship between P and S (H-series)*

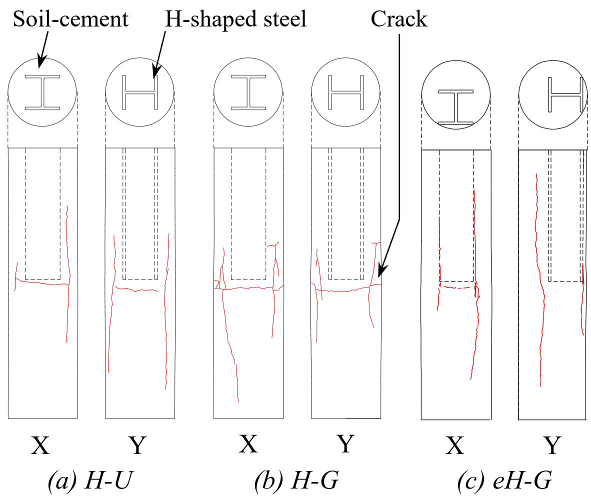


*Figure 11. Sketches of pile after loading test (H-series)*

The increase in bearing strength due to soil confinement stress offsets the decrease in bearing strength caused by the eccentricity of the steel. Consequently, the $P_P$ values for eH-G and eC-G are higher than those for H-U and C-U. Relative displacement occurs after $P_P$ was reached and the pile head load gradually increases. The $P_R$ values for eH-G and eC-G are comparable to those for H-G and C-G, indicating a smaller effect of H-shape steel eccentricity compared to that in the S-series.

In the H- and C-series piles, soil-cement wedges formed at the tips of the steel and splitting failure initiated from the wedge tips. Note that the wedge shape varied depending on the bearing cross section.

Figure 14 compares the experimental results obtained with and without eccentricity in the steel. $\overline{P_P}$ and $\overline{P_R}$ were calculated by dividing the $P_P$ and $P_R$ for each series by the ratio of the unconfined compressive strength $q_u$ to the target strength of 2.0 N/mm$^2$. Except for the H-series, $\overline{P_P}$ tends to decrease due to steel eccentricity. That is, the pile strength decreases because the bond strength, shear strength, and bearing strength decrease due to steel eccentricity. Except for the C-series, steel eccentricity tends to increase $\overline{P_R}$. This increase is particularly pronounced in the S-series, resulting from the expansion of the shear failure range due to the eccentricity of the steel shown in Figure 9.

Figure 15 shows the safety factors $S_U$ and $S_G$ for vertical bearing capacity evaluation. $S_U$ is the value obtained by dividing the $\overline{P_P}$ for O-G and eO-G, respectively, by the sum of the $\overline{P_P}$ for S-U and C-U. $S_G$ is the value obtained by dividing the $\overline{P_P}$ for O-G and eO-G, respectively, by the sum of the $\overline{P_P}$ for S-G and C-G. In other words, this value represents the ratio of the pile strength to the sum of the bond strength, shear strength, and bearing strength. A safety factor exceeding 1 indicates that the pile body strength can be safely (conservatively) evaluated based on the sum of the bond strength, shear strength, and bearing strength. $S_G$ is approximately 0.8 to 0.9.

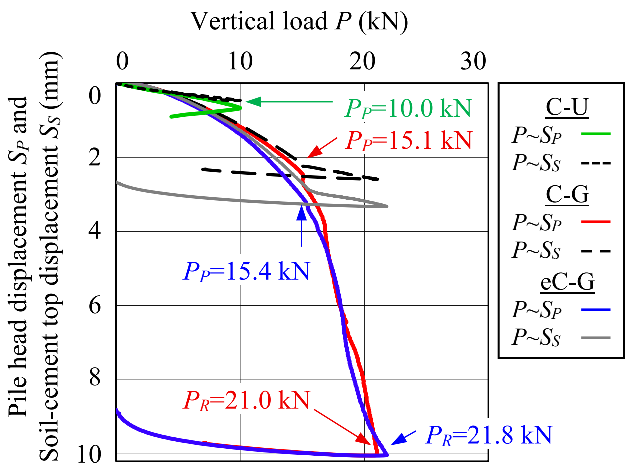


Figure 12. Relationship between P and S (C-series)

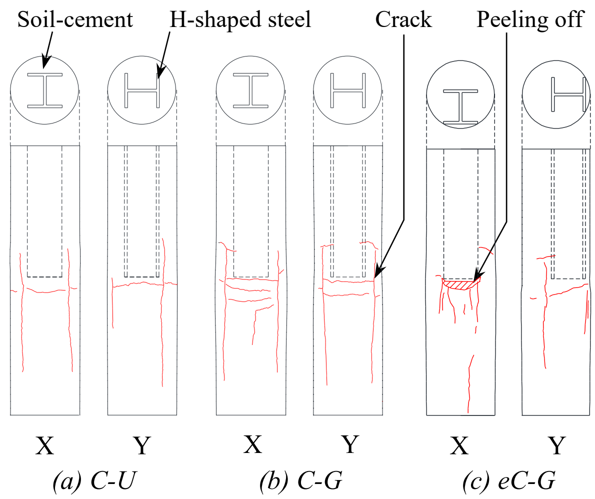


Figure 13. Sketches of pile after loading test (C-series)

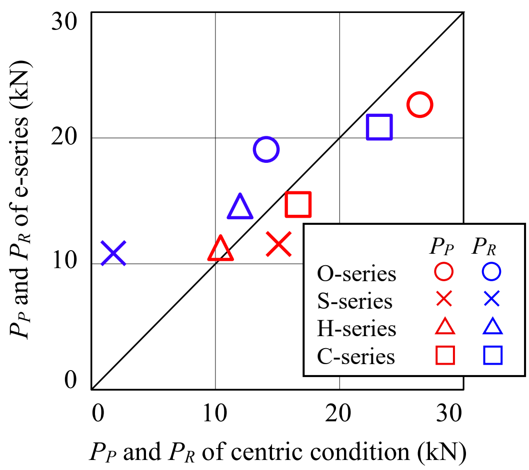


Figure 14. Effect of eccentricity

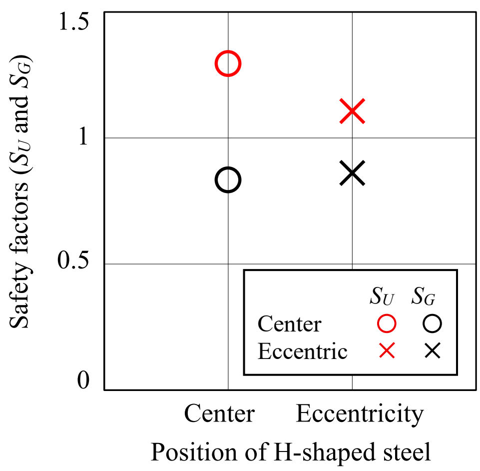


Figure 15. Safety factors for vertical bearing capacity evaluation

This indicates that the compressive stress transmitted from the bonded section affects the bearing section and that the sum of the bond strength, shear strength, and bearing strength cannot be used to safely evaluate the vertical bearing capacity. This has also been pointed out in research by Usami et al. (2001) on cast-in-place concrete piles. $S_U$ is approximately 1.1 to 1.3. The increase in pile strength due to soil compaction stress offsets the decrease in pile strength caused by the eccentricity of the steel. This demonstrates that the vertical bearing capacity can be safely evaluated by simply summing the bond strength, shear strength, and bearing capacity in the unconfined condition.

## 5 CONCLUSION

In this study, model piles were subjected to vertical loading tests using a pressurized tank. The effect of H-shaped steel beam eccentricity on vertical bearing capacity was examined based on experimental results. The findings can be summarized as follows.

- Eccentricity in the steel reduces the bond strength, shear strength, and bearing capacity of soil-cement, consequently decreasing pile strength.
- Eccentricity alters the failure mode between the steel and soil-cement. The expanded shear failure zone due to eccentricity increases the residual shear strength.
- Although eccentricity reduces the pile strength, the increase in pile strength due to ground confinement stress offsets this reduction.

## REFERENCES


Abe, K. and Mano, H. (2018). ソイルセメント連続壁内の H 形鋼の鉛直支持力(その 1)原位置載荷試験. Bearing capacity of h-shaped steel in soil cement retaining wall (Part 1: in-situ vertical loading tests). The 53rd Japan National Conference on Geotechnical Engineering, pp. 1431–1432. (in Japanese)

Architectural Institute of Japan (2017). *AIJ Recommendations for Design of Earth Retaining for Excavation*. Fourth Edition, pp. 130–133.

Ikeuchi, K., Usami, T., and Miyauchi, Y. (2024). 埋め込まれた鉄骨柱の先端のみが補強された杭頭部の軸耐力. Axial Strength of Pile Head Embedded with Steel Column Considering Cover Concrete Thickness and Column Eccentricity (Transactions of AIJ), Vol.89, No.815, pp.121–127. (in Japanese) https://doi.org/10.3130/aijs.89.121

Kiritani, R., Shimomura, S., Aoyama, A. and Nomura, Y. (2025). ソイルセメント山留め壁の鉛直支持力に及ぼす地盤による拘束の影響に関する模型実験. Study on Confined Effect by Ground on Vertical Bearing Capacity of Soil-cement Retaining Wall Using Model Tests (Transactions of AIJ), Vol.90, No.829, pp.354–364. (in Japanese) https://doi.org/10.3130/aijs.90.354

Satake, K., Uchii, E., Otsuka, S., Fujiwara, T. and Takeuchi, Y. (2003). ソイルセメント本設杭工法の開発(その 4 ソイルセメントと芯材間の荷重の伝達). Development of a permanent soil cement mixing pile, part 4 transmission of load between soil cement & h-steel. Summaries of technical papers of annual meeting, Architectural Institute of Japan, Structure-I, pp. 677–678. (in Japanese)

Sato, T., Ikawa, N., Uchii, E., Kono, M. and Hidaka, Y. (2003). ソイルセメント本設杭工法の開発(その 5 H 形鋼先端部の極限支持力). Development of a permanent soil cement mixing pile, part 5 ultimate bearing capacity of h-steel. Summaries of technical papers of annual meeting, Architectural Institute of Japan, Structure-I, pp. 679–680. (in Japanese)

Taya, Y. and Yamanaka, R. (2021). ソイルセメント地中連続壁工法におけるソイルセメントと芯材の付着力・スタッド耐力. Evaluation for adhesion of h-section steel and stud resistance to soil-cement by trench cutting re-mixing deep wall method, Summaries of technical papers of annual meeting, Architectural Institute of Japan, Structure-I, pp. 365–366. (in Japanese)

Tsuchiya, T., Hamada, J., Okamoto, K., Kawai, E. and Usami, T. (2004). 掘削土再利用連壁の本設杭利用の研究(その 1)実験概要とソイルセメント中の H 形鋼の室内押抜き実験. Study on piles utilizing of continuous-walls using recycled mud (part 1: outline of experiment), summaries of technical papers of annual meeting, Architectural Institute of Japan, Structure-I, pp.561–562. (in Japanese)

Usami, T., Kei, T., Aoki, M., Hirai, Y. and Ito, H. (2001). 鉄骨柱から場所打ちコンクリート杭頭部への軸力伝達に関する実験的研究. Axial Force Transmission from Steel Column to Cast-in-place Concrete Pile Head, Journal of Structural and Construction Engineering (Transactions of AIJ), Vol.66, No.547, pp.105–112. (in Japanese) https://doi.org/10.3130/aijs.66.105_3

Watanabe, K., Wada, K., Yokoyama, T. and Hirata, M. (2021). 本設杭として用いるソイルセメント柱列壁の杭体における付着性能評価. Evaluation of bond performance on pile body of soil-cement mixing wall used as permanent pile, Journal of Structural Engineering, Vol.67B, pp.445–452. (in Japanese)